of largest shielding deviates by as much as 20° from the amide bond. A second principal axis (the *least* shielded one) is dictated by symmetry to be perpendicular to the molecular plane. This symmetry is broken for the twisted form of GG. In both the monomer and the monohydrate twisted forms, the least shielded direction is calculated to deviate by ~5° from the normal of the peptide plane. Remember we find a deviation of ~11° between $\vec{e}_X^{CS,N}$ and $\vec{n}_{peptide}$ in NAV.

Upon hydration, the ab initio calculations yield an increase of $\Delta\sigma$ by ~11 ppm and a decrease of σ^{iso} by ~3 ppm. In Table III we list the results of the ab initio calculation for the monohydrate in conformation I, for which a linear hydrogen bond between the amide nitrogen and the water oxygen and a distance $|\overrightarrow{NO}| = 2.859$ Å were assumed. The calculated numbers are in good agreement with the experimental results for AA and NAV. Note, the increase of σ^{iso} and $\Delta\sigma$ with decreasing NO distance.

The ab initio calculation for the planar monohydrate predicts the direction of largest shielding to be parallel to the NH bond. If a nonlinear hydrogen bond is assumed ($\angle(\overrightarrow{NO},\overrightarrow{NO}) \approx 15°$), the direction of largest shielding is found to deviate from $\overrightarrow{NH}$ by about 10°. For NAV, where $\angle(\overrightarrow{NH},\overrightarrow{NO}) \approx 20°$, we measured a deviation between $\vec{e}_Z^{CS,N}$ and $\overrightarrow{NH}$ of ~9°. Overall, the results of the ab initio calculations are in good agreement with our experimental results.

5. Conclusions

We have shown that it is possible to measure the CS tensor of the amide hydrogen in the model peptide NAV by ^{2}H-NMR on single-crystal samples. Our measurements also yield the CS tensor of the carboxyl hydrogen and the QC tensors of both the amide and carboxyl deuterons. All are in good agreement with previous experimental and theoretical results obtained from comparable compounds.

Our main purpose was to examine the relationship of the amide hydrogen CS tensor to the structure of the peptide. The CS tensor we obtained from the amide hydrogen in NAV is consistent with the results of a previous, but less complete, experimental study of acetanilide[8] and the recent ab initio calculations of glycylglycine.[9] The results of our work and these two studies imply that there is a close correlation between the strength of the N-H···O hydrogen bond and the values of σ^{iso} and $\Delta\sigma$. A similar correlation is well established for O-H···O hydrogen bonds.

With respect to the orientation of the CS tensor of the amide hydrogen in NAV, we find that the most shielded eigenvector is close to the NH bond, while the least shielded is close to the normal of the peptide plane. The observed deviations of 9° and 11°, respectively, are larger than the experimental error. We attribute these deviations to the lack of extended mirror symmetry in the NAV molecule (the dihedral angle between the peptide and the carboxyl plane is ~41°) and to the nonlinearity of the N-H···O hydrogen bond. The eigenvectors of the QC tensor of the amide deuteron are much more intimately related to the local molecular structure of the peptide than are those of the CS tensor: $\vec{e}_Z^{QC,N}$ deviates from $\overrightarrow{NH}$ by only 1.8°, and $\vec{e}_X^{QC,N}$ from $\vec{n}_{peptide}$ by only 0.9°.

Acknowledgment. We thank A. Heuer for supplying computer fit routines, D. Theimer for his initial help in the measurements, and D. B. Chestnut for providing his CS tensor data for glycylglycine prior to publication. R.G. gratefully acknowledges the Max-Planck-Gesellschaft for support while in Heidelberg. J.R. was supported by a postdoctoral fellowship from the NRC of Canada. The research at the University of Pennsylvania was supported by Grants R01 GM-24266, R01 GM-29754, and R24 RR-05976 from the National Institutes of Health.

Electron Affinities, Enthalpy, and Entropy of Electron Attachment of Several η^4-(Olefin)Fe(CO)$_3$ Complexes and Electron-Transfer Kinetics

Paul Sharpe and Paul Kebarle*

Contribution from the Department of Chemistry, University of Alberta, Edmonton, Canada T6G 2G2. *Received July 7, 1992*

Abstract: The energies $\Delta H°_a$ and $\Delta G°_a$ and the entropy $\Delta S°_a$ for the electron attachment (capture) process e + B = B$^-$ were determined for the olefin iron tricarbonyls, where the olefin = 1,3-butadiene (Bd), 1,3-cyclohexadiene (CHD), 1,3,5-cycloheptatriene (CHT), and cyclooctatetraene (COT). Data were obtained also for trimethylenemethane-Fe(CO)$_3$ and cycloheptatriene-Cr(CO)$_3$. The determinations were made with a pulsed electron high pressure mass spectrometer which allows measurement of electron-transfer kinetics and equilibria: A$^-$ + B = A + B$^-$. Compounds A were reference compounds with known $\Delta H°_a$, $\Delta G°_a$, and $\Delta S°_a$. The thermodynamic and kinetic data indicate that for the Ol-Fe(CO)$_3$, electron capture leads to a reduction of hapticity from 4 to 2 for Ol = Bd, CHD, CHT but a change over occurs for COT where the electron enters an orbital largely localized on the olefin.

Introduction

In previous work[1,2] we reported measurements of the electron attachment (capture) free energy, $\Delta G°_a$, enthalpy, $\Delta H°_a$, and entropy, $\Delta S°_a$, involving η^4-1,3-butadiene iron tricarbonyl (BdFe(CO)$_3$). These relate to the gas phase reaction where BdFe(CO)$_3$ = B.

$$e + B = B^- \quad (1)$$

The electron attachment energies and entropy were obtained from measurements of gas phase electron transfer equilibria 2 where A is a reference compound with known $\Delta G°_a$, $\Delta H°_a$, and $\Delta S°_a$.

$$A^- + B = A + B^- \quad (2)$$

The equilibria 2 were measured with a pulsed electron high pressure mass spectrometer, PHPMS, using apparatus, techniques, and methodology which have been described in previous work.[3,4]

(1) Dillow, G. W.; Nicol, G. Kebarle, P. *J. Am. Chem. Soc.* **1989**, *111*, 5465.
(2) Dillow, G. W.; Kebarle, P. *J. Am. Chem. Soc.*, in press.
(3) Kebarle, P. In *Techniques of Chemistry*; Saunders, W. H., Farrar, J. M. Eds.; Wiley-Interscience: New York, 1988.
(4) Kebarle, P.; Chowdhury, S. *Chem. Rev.* **1987**, *87*, 513.

0002-7863/93/1515-782$04.00/0

BdFe(CO)$_3$ is interesting because it is an 18-electron species. The LUMO of BdFe(CO)$_3$ is thus expected to be of relatively high energy and on this basis the compound may not be able to form a stable radical anion in the gas phase or solution. However, the radical anion has been generated in solution by electrochemical, one-electron reduction of BdFe(CO)$_3$. It was established that the reduction was reversible, and this is consistent with no loss of one of the CO groups and no complete separation of the Bd group on formation of the radical anion. Krusic et al.[5] were able to obtain an ESR spectrum after the reduction, which consisted of a not fully resolved triplet of doublets, as would be expected for the interactions of an unpaired electron, with two equivalent and one non-equivalent hydrogen nuclei. This was strong evidence that the unpaired electron is located largely on the Fe and interacts with the tree H atom nuclei of only one of the vinyl groups in 1,4-butadiene. Thus, a reduction of the hapticity of the butadiene from η^4 to η^2 should have occurred as indicated in reaction 3. The

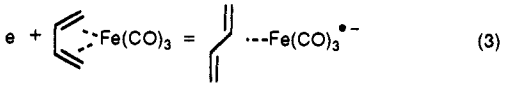

(3)

capture of the extra electron thus has led to a decoordination of the η^4-BdFe(CO)$_3$ to η^2-BdFe(CO)$_3^-$ where the radical anion complex is a 17-electron species and the 18-electron rule is not violated.

In gas phase therminology process 3 could be considered as a dissociative electron capture where the dissociated (vinyl) group is not lost because it remains attached to the other still bonded (vinyl) group.

While the evidence for reaction 3 by Krusic et al.[5] was good, the interpretation of the ESR spectrum was not "iron clad" and therefore in our previous work[1,2] we found it of interest to examine whether the thermodynamic quantities for electron attachment in the gas phase would be consistent with process 3. The thermodynamic data obtained[2] are shown below:

$$\text{BdFe(CO)}_3: \quad \Delta G°_a = -24.6;\ \Delta H°_a = -20.7;\ \Delta S°_a = +10.3 \tag{4}$$

where $\Delta G°_a$ is for $T = 373$ K, $\Delta H°$ and $\Delta G°$ are in kcal/mol, and $\Delta S°$ is in cal mol^{-1} K^{-1}. In the evaluation of $\Delta G°_a$, $\Delta H°_a$, and $\Delta S°_a$ the stationary electron convention[7,8] was used.

The $\Delta S°_a = 10.3$ cal mol^{-1} K^{-1} value is very much larger than the usually[4,8] observed change to −2 to +2 cal mol^{-1} K^{-1} for electron attachment which is nondissociative. The large positive entropy is a clear sign for a very large loosening in the relative motions between two (or more) heavy groups of the BdFe(CO)$_3^-$ radical anion. The most likely change is that in the relative motions between Bd and Fe(CO)$_3$. Although an accurate prediction of the $\Delta S°_a$ on the basis of statistical mechanics evaluation of the entropy terms due to changes of vibrational frequencies on electron capture could not be obtained due to lack of supporting data, it was concluded[2] that the observed large $\Delta S°_a = 10.3$ cal deg^{-1} mol^{-1} is entirely consistent with the reduced bonding indicated in reaction 3.

In the electron capture reaction 3, a lower lying LUMO is created by a bond dissociation reaction. Thus the higher exothermicity of electron capture in the new low energy LUMO has to be purchased at the cost of an endothermic bond cleavage. Such a trade off will generally not lead to high electron capture exothermicities and the EA $\approx -\Delta H_a$ of 20.7 kcal/mol is fairly low as far as electron affinities go.[4]

The olefin–Fe(CO)$_3$ complexes, where the olefin = cyclohexadiene, cycloheptatriene, and cyclooctatriene, together with the BdFe(CO)$_3$, represent compounds that have been much studied in the condensed phase.[9-11] For structures and abbreviated names used in this work see I–IV below.

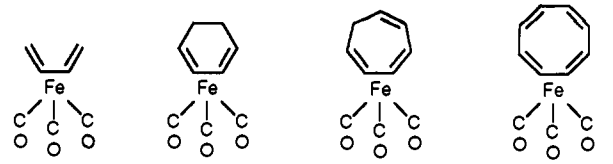

BdFe(CO)$_3$ (I) (CHD)Fe(CO)$_3$ (II) (CHT)Fe(CO)$_3$ (III) (COT)Fe(CO)$_3$ (IV)

Although the bonding in the neutral compounds is of the same type in I–IV, changes in the geometry and energies of the π^* orbitals of the olefins can lead to significant differences in the strength of the olefin–Fe(CO)$_3$ bonding and in the LUMO energy. Therefore, in the present work we determined the electron attachment energies and entropies for the CHD, CHT, and COT iron carbonyl compounds. Data were obtained also for trimethylenemethane iron tricarbonyl, TMMFe(CO)$_3$, and the (CHT)Cr(CO)$_3$ compounds. As will be seen, the results are informative and provide interesting insights concerning the orbital reorganization associated with the electron capture by these compounds.

Experimental Details and Methodology

Apparatus and Measurements. The measurements of the electron transfer equilibria reaction 2 were performed with the pulsed electron high pressure mass spectrometer which has been described in detail.[3] The techniques used with the organometallic compounds were very similar to those in the previous work[2] involving BdFe(CO)$_3$. Therefore, only information of special relevance to the present work will be given here.

The organic reference compounds, see Figure 1, were from commercial sources as in the earlier work.[2,4] Their purity was checked by obtaining the electron capture negative ion mass spectra. These generally showed only the molecular anion. In rare cases, fragments were observed also and these were demonstrably due to the parent compound. BdFe(CO)$_3$, (CHD)Fe(CO)$_3$, (COT)Fe(CO)$_3$, and CHTCr(CO)$_3$ were obtained from commercial sources. A sample of (CHT)Fe(CO)$_3$ was generously donated by Dr. J. Takats from this Department. The (TMM)Fe(CO)$_3$ was synthesized following literature preparations.[12]

BdFe(CO)$_3$, (CHT)Fe(CO)$_3$, and (TMM)Fe(CO)$_3$ are air sensitive. Volumetric solutions of these compounds in benzene were stored under argon in Schlenk tubes without any apparent deterioration. The gas mixtures consisting of 700 Torr of methane and the two reactants A and B, see eq 2, were prepared in a 5-L storage bulb of the thermostated gas handling plant.[3] A and B were introduced by injecting benzene or toluene solutions of the compounds with a microsyringe, through a septum, into the 5-L bulb. The temperature of the bulb was kept high enough to ensure complete evaporation of A and B. The organometallic compounds are easily thermally decomposed and therefore the temperature of the bulb was kept below 90 °C. At such temperature no decomposition occurred. This was established by measuring equilibrium constants with the same reaction mixture before and after the mixture had been stored over a period of hours in the heated bulb and finding the constant unchanged.

Thermochemical Results. The equilibrium constants, K_{el}, for the electron transfer reaction

$$A^- + B = A + B^-$$

where A are reference compounds with known electron attachment energies $\Delta G°_a$ and $\Delta H°_a$ and B are the present organometallic compounds, were determined by measuring with the mass spectrometer the intensities of the ions A$^-$ and B$^-$ after equilibrium was achieved.[2-4] The free energies obtained with eq 5 from measurements in the present work are shown in Figure 1.

$$\Delta G°_{el} = -RT \ln K_{el} \tag{5}$$

(5) Krusic, P. J.; San Fillipo, J., Jr. *J. Am. Chem. Soc.* **1982**, *104*, 2645.
(6) El Murr, N.; Payne, J. D. *J. Chem. Soc., Chem. Commun.* **1985**, 162.
(7) The stationary electron convention[8] neglects the translational entropy of the electron, which when in a large box, as is the case here, follows Boltzman statistics. The stationary electron convention has the advantage of dealing only with the changes due to the process B → B$^-$, see eq 1, which is of primary interest here.
(8) Chowdhury, S.; Heinis, T.; Grimsrud, E. P.; Kebarle, P. *J. Phys. Chem.* **1986**, *90*, 2747.
(9) Deganello, G. *Transition Metal Complexes of Cyclic Polyolefins*; Academic Press: New York 1979.
(10) LiShing Man, L. K. K.; Renvers, J. G. A.; Takats, J.; Deganello, G. *Organometallics* **1983**, *2*, 28.
(11) Albright, T. A.; Geiger, W. E.; Mozaczewski, J.; Tulyathan, B. *J. Am. Chem. Soc.* **1981**, *103*, 4787.
(12) Ehrlich, K.; Emerson, G. F. *J. Am. Chem. Soc.* **1972**, *94*, 2464.

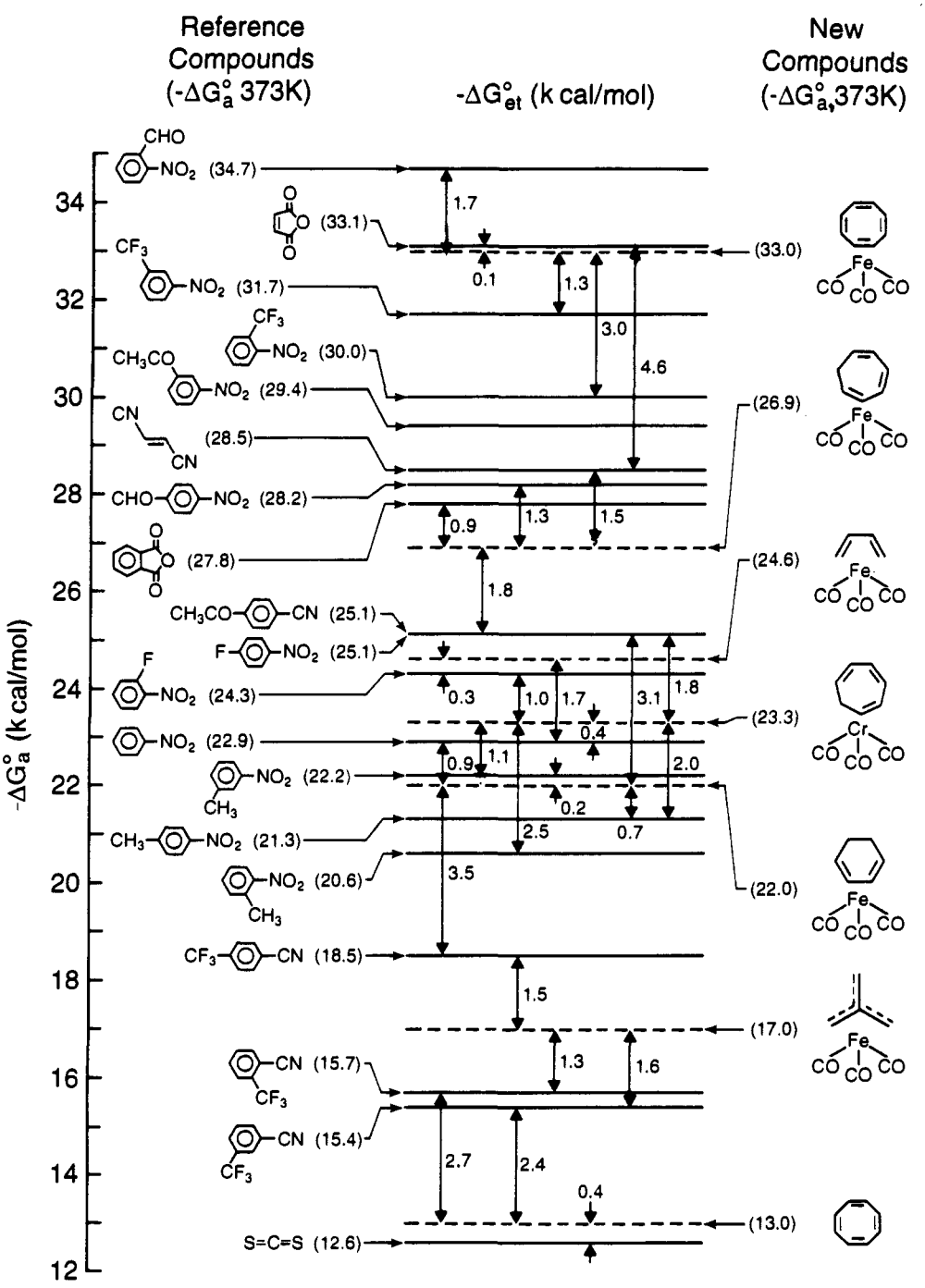

Figure 1. Summary of free changes, ΔG°_{et}, for the electron transfer reactions $A^- + B = A + B^-$, where A are reference compounds with known electron attachment (capture) free energies, $-\Delta G^\circ_a(A)$, and B are the organometallic compounds with unknown $\Delta G^\circ_a(B)$. ΔG°_{et} are presented in a scale which reveals the internal consistency of the data.

The ΔG°_{et} obtained with different reference compounds are combined into a ΔG°_{et} scale which provides relative ΔG°_a values since eq 6 holds:

$$\Delta G^\circ_{et} = \Delta G^\circ_a(B) - \Delta G^\circ_a(A) \quad (6)$$

The known $\Delta G^\circ_a(A)$ lead then to (obsolute) $\Delta G^\circ_a(B)$ values of the organometallic compound of interest. As is evident from Figure 1, multiple measurements involving different A compounds and the same B lead to redundant determinations whose consistency is generally better than 0.3 kcal/mol. Thus, four ΔG°_{et} with four different reference compounds A lead to $\Delta G^\circ_a(BdFe(CO)_3)$ values which are consistent to within less than 0.1 kcal/mol, see Figure 1. However, the ΔG°_a values of the reference compounds may be uncertain to within 1 kcal/mol and therefore we estimate that the $\Delta G^\circ_a(B)$ values are uncertain to ±1.5 kcal/mol.

The ΔH°_{et} and ΔS°_{et} were obtained from measurements of K_{et} at different temperatures and used to construct van't Hoff plots whose slope provides ΔH°_{et} and the intercept ΔS°_{et}. An example of such van't Hoff plots involving B = $(CHT)Cr(CO)_3$ and three different reference compounds A is shown in Figure 2.

The ΔH°_{et} and ΔS°_{et} obtained from the van't Hoff plots are given in Table I. Also given are the known[4,13-15] values ΔH°_a and ΔS°_a for the reference compounds A. The $\Delta H^\circ_a(B)$ and $\Delta S^\circ_a(B)$ obtained with an equation analogous to eq 6 are also shown in Table I. As can be seen, $\Delta H^\circ_a(B)$ and $\Delta S^\circ_a(B)$ when obtained from electron transfer involving more than one reference compound A are consistent to within ~0.5 kcal/mol for ΔH_a and ~1 cal deg^{-1} mol^{-1} for ΔS°_a. The error in the resulting $\Delta H_a(B)$ data is estimated at ±2 kcal/mol and that for $\Delta S^\circ_a(B)$ is ±3 cal deg^{-1} mol^{-1}.

(13) Chowdhury, S.; Heinis, T.; Grimsrud, E. P.; Kebarle, P. *J. Phys. Chem.* **1986**, *90*, 2747.
(14) Chowdhury, S.; Kebarle, P. *J. Am. Chem. Soc.* **1986**, *108*, 5453.
(15) Chowdhury, S.; Kishi, H.; Dillow, G. W.; Kebarle, P. *Can. J. Chem.* **1989**, *67*, 603.

Table I. Electron Attachment Enthalpies (ΔH_a) and Entropies ($\Delta S°_a$) for the Organometallic Compounds B, Obtained from Electron-Transfer Equilibria $A^- + B = A + B^-$ with Reference Compounds A[a]

					A		*B*[g]	
B	A[b]	$\Delta G°_{et}$ (373 K)	$\Delta H°_{et}$	$\Delta S°_{et}$	$\Delta H°_a$	$\Delta S°_a$	$\Delta H°_a$	$\Delta S°_a$
(Bd)Fe(CO)$_3$	2F-NB[c]	−0.4	+4.1	+11.9	−24.8	−1.6	−20.7	10.3
(Bd)Fe(CO)$_3$	NB[c]	−1.6	+2.5	+11.0	−23.2	−1.0	−20.7	10.0
(CHD)Fe(CO)$_3$	4CF$_3$-NB[d]	−3.4	−0.1	+8.8	−17.5	+2.6	−17.6	+11.4
(CHT)Fe(CO)$_3$	C$_2$H$_2$(CN)$_2$[d]	+1.6	+6.1	+11.9	−28.8	−1.0	−22.7	+10.9
(CHT)Fe(CO)$_3$	4CH$_3$CO-BN[d]	−1.9	+2.9	+13.0	−25.9	−2.0	−23.0	+11.0
(CHT)Fe(CO)$_3$	4CHO-BN[e]	+1.2	+6.4	+13.8	−28.9	−2.0	−22.5	+11.8
(COT)Fe(CO)$_3$	mal anh[c]	+0.1	+4.0	+10.6	−33.2	−0.4	−29.2	+10.2
(COT)Fe(CO)$_3$	3CF$_3$-NB[c]	−1.3	+2.6	+10.4	−32.6	−2.5	−30.0	+7.9
(COT)Fe(CO)$_3$	3CH$_3$CO-NB[f]	−3.6	+0.1	+10.0	−30.6	−3.0	−30.5	+7.0
(CHT)Cr(CO)$_3$	2CH$_3$-NB[c]	−2.5	0.0	+6.4	−21.3	−1.6	−21.3	+4.8
(CHT)Cr(CO)$_3$	3CH$_3$-NB[c]	−1.3	+1.5	+7.4	−22.8	−1.7	−21.3	+5.7
(CHT)Cr(CO)$_3$	4CH$_3$-NB[c]	−2.0	+0.5	+6.6	−22.0	−2.0	−21.5	+4.6

[a] Free energies and enthalpies are in kcal mol^{-1}, entropies in cal mol^{-1} K^{-1}. [b] Notations used: NB = nitrobenzene; BN = benzonitrile; *t*-C$_2$H$_2$(CN)$_2$ = fumaronitrile; mal anh = maleic anhydride. [c] $\Delta H°_a$ and $\Delta S°_a$ taken from ref 13. [d] $\Delta H°_a$ and $\Delta S°_a$ taken from ref 14. [e] $\Delta S°_a$ estimated to be −2 cal K^{-1} mol^{-1}, $\Delta H°_a$ obtained from $\Delta S°_a$, and $\Delta G°_a$ = −28.9 kcal/mol at 373 K from ref 14. Estimate of $\Delta S°_a$ based on comparison with available $\Delta S°_a$ of other substituted benzonitriles and nitrobenzenes.[4,13-15] [f] From ref 15. [g] Estimated error ±2 kcal/mol for $\Delta H°_a$(B) and ±3 cal deg^{-1} mol^{-1} for $\Delta S°_a$(B).

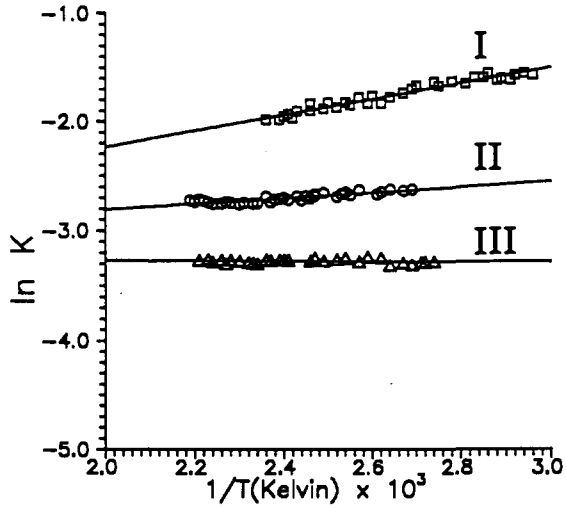

Figure 2. Some representative van't Hoff plots of electron transfer equilibrium constants K_{et} for several reactions: (I) CHTCr(CO)$_3^-$ + 3-CH$_3$NB = CHTCr(CO)$_3$1− + 3-CH$_3$NB$^-$; (II) CHTCr(CO)$_3^-$ + 4-CH$_3$NB; (III) CHTCr(CO)$_3^-$ + 2-CH$_3$NB. For results from slope and intercept see Table I.

The temperature range over which the electron transfer equilibria, eq 2, could be measured was limited to 50–120 °C. The low-temperature limit was imposed by volatility requirements, while at high temperatures other reaction channels and particularly CO loss from the radical anion were found to occur. A detailed study of this reaction for BdFe(CO)$_3^-$ was presented in our previous study.[2] The Cr complex (CHT)Cr(CO)$_3^-$ was found to be more stable with respect to CO loss than the iron complexes and showed no sign of thermal decomposition up to 170 °C, the highest temperature used.

Electron transfer equilibria involving trimethylenemethane–Fe(CO)$_3$, (TMM)Fe(CO)$_3$, could be performed only at low temperature (~70 °C) and therefore van't Hoff plots could not be obtained for this compound. After the initial formation of (TMM)Fe(CO)$_3^-$, in bath gas containing only this compound, the radical anion was found to decay fairly rapidly while ions of *m/z* 388 and 360 were formed. These ionic reaction products have been observed previously by Wang and Squires,[16] who proposed reactions 7 to explain their formation.

$$(C_4H_6)Fe(CO)_3^- \xrightarrow{a} Fe_2(C_4H_6)_2(CO)_6^- \qquad (C_4H_6)Fe(CO)_3^- \xrightarrow{b} Fe_2(C_4H_6)_2(CO)_5^- + CO \qquad (7)$$

The electron transfer equilibria 2 could be measured only at very low pressures of (TMM)Fe(CO)$_3$, typically 10^{-5} Torr, which is ~10 times lower than normally used pressures. At this low pressure, the dimerization reactions were largely suppressed. The reaction channel 7b could be further suppressed by the addition of ~0.25 Torr of CO to the ion source. Considerably higher CO pressures were not useful, since the CO reacted with (TMM)Fe(CO)$_3^-$ leading to Fe(CO)$_4^-$ product. Another possible cause for the appearance of Fe(CO)$_4^-$ is the presence of Fe(CO)$_5$, a common impurity in steel cylinders containing CO.

Kinetic Measurements. The rate constants for reaction 2 ($A^- + B = A + B^-$) were determined with the usual methodology.[2-4] To correct for ion loss by diffusion, the intensities of A^- and B^- were expressed as percent of the total $A^- + B^-$ intensity.[3] These "normalized" intensities were used in two types of plots in order to extract the rate constants. For large exothermicities where reaction 2 goes to completion a plot of the logarithm of the normalized intensity of A^- versus *t* gave a straight line with a slope equal to $\nu_2 = k_2[B]$. The rate constant k_2 could then be extracted from the known concentration of B.

At low exoergicities, where the reaction reached equilibrium, the forward rate constant was obtained with the standard, integrated rate equation for a reversible first order reaction:

$$\ln \frac{(x_e - x_0)}{(x_e - x)} = \frac{100\nu_2}{x_e} t$$

The ion intensity of B^- is x_0 at $t = 0$, x at $t = t$, and x_e at equilibrium. The total ion intensity of A^- plus B^- is 100.

Plots of $\ln (x_e - x_0)/(x_e - x)$ versus *t* gave good straight lines with zero intercept, and the slope $(100\nu_2/x_e)$ and the known x_e were used to evaluate ν_2.

Discussion

a. Electron Capture Thermochemistry and Orbital Reorganization. The average electron attachment enthalpies $\Delta H°_a$ and entropies $\Delta S°_a$ for the olefin Fe(CO)$_3$ compounds, from Table I, are shown in Table II and Chart I, together with the corresponding structure of the neutral compounds. For the olefin ligand series CHD, BD, CHT, and COT, one observes a gradual increase of $-\Delta H_a$. The increase is particularly large, 7 kcal/mol, from CHT to COT, larger than the total increase for the preceding compounds: CHD, BD, CHT. The entropy changes, $\Delta S°_a$, remain quite similar up to CHT, and then a significant drop of 3 cal K^{-1} mol^{-1} is observed between CHT and COT. These data indicate a possible special change between CHT and COT.

This simple analysis can be extended on the basis of the thermodynamic cycle shown below.

$$\begin{array}{ccc} Ol + Fe(CO)_3 + e & \xrightarrow{\Delta H_a(Fe(CO)_3)} & Ol + Fe(CO)_3^- \\ \uparrow -D(Ol\text{-}Fe(CO)_3) & & \downarrow D(Ol\text{-}Fe(CO)_3^-) \\ Olfe(CO)_3 + e & \xrightarrow{\Delta H_a(Olfe(CO)_3)} & Olfe(CO)_3^- \end{array} \qquad (8)$$

Ol stands for olefin and D(Ol–Fe(CO)$_3$) stands for the energy required for the complete dissociation of the olefin from the

(16) Wang, D.; Squires, R. R. *Organometallics* **1987**, *5*, 905.

Table II. Summary of Thermochemical Data[a] for Electron Attachment to Organometallic Compounds and Cyclooctatetraene

	$\Delta G°_a$(373 K)	$\Delta H°_a$	$\Delta S°_a$
(Bd)Fe(CO)$_3$	−24.6	−20.7	10.2
(CHD)Fe(CO)$_3$	−22.0	−17.6	11.4
(CHT)Fe(CO)$_3$	−26.9	−22.7	11.2
(COT)Fe(CO)$_3$	−33.0	−29.7	8.7
(CHF)Cr(CO)$_3$	−23.3	−21.4	5.0
(TMM)Fe(CO)$_3$	−17.0[b]		
cyclooctatetraene	−13.0		

[a] Average values for $\Delta G°_a$ from Figure 1, estimated error ±1.5 kcal/mol. Average values for $\Delta H°_a$ and $\Delta S°_a$ from Table I. Estimated errors ±2 kcal/mol for $\Delta H°_a$ and ±3 cal K^{-1} mol^{-1} for $\Delta S°_a$. Stationary electron convention used. [b] Data obtained at 70 °C.

Chart I

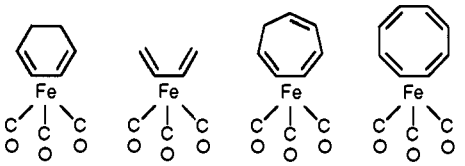

$-\Delta H°_a$, kcal/mol	17.6	20.7	22.7	29.7
$\Delta S°_a$, cal/ K^{-1} mol^{-1}	11.4	10.2	11.2	8.7

Fe(CO)$_3$ group. The relationships in the cycle can be expressed by eq 9a. The electron affinity of Fe(CO)$_3$ has been measured, with the laser induced photodetachment technique, by Engleking and Lineberger,[17] EA(Fe(CO)$_3$) = 41.5 ± 4.6 kcal/mol. Since EA ≈ $-\Delta H_a$ (see detailed comparison[8] for the case of SO_2), the Lineberger value can be used in the cycle and leads to eq 9b.

$$D(\text{Ol–Fe(CO)}_3^-) - D(\text{Ol–Fe(CO)}_3) = \Delta H_a(\text{OlFeCO}_3) - \Delta H_a(\text{Fe(CO)}_3) \quad (9a)$$

$$= \Delta H_a(\text{OlFeCO}_3) + 41.5 \text{ (kcal/mol)} \quad (9b)$$

Expression 9 provides the difference between the bond energy in the neutral and the radical anion and thus a measure of the weakening of the bonding between the olefin and Fe(CO)$_3$ associated with the accommodation of the extra electron. The actual D(Ol–Fe(CO)$_3$) − D(Ol–Fe(CO)$_3^-$) values (kcal/mol) obtained with eq 9 are given below each structure

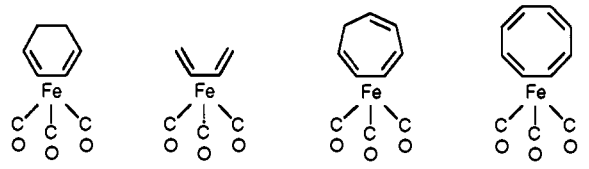

24 21 19 11.8

The bond energy difference is approximately the same for Ol = Bd, CHD, CHT; however, a large drop is experienced for COT. This means that the decrease in bonding required by the reorganization in order to accommodate the extra electron is by far the smallest for cyclooctatetraene.

The bond energies D(Bd–Fe(CO)$_3$) = 56.0 ± 8 kcal/mol and D(COT–Fe(CO)$_3$) = 50.9 ± 8.4 kcal/mol are available from recent determinations.[18] Therefore one can evaluate with eq 9b and the available ΔH_a for these compounds the corresponding bond energies of the negative ions: D(Bd–Fe(CO)$_3^-$) ≈ 35.2 kcal/mol and D(COT–Fe(CO)$_3^-$) = 39.5 kcal/mol. These figures show that the bond energy in the negative ion relative to that in the neutral is 62.5% for Bd and 76.6% for COT. The reduction of the bond energy to close to half of the value in the neutral, observed for Bd, is consistent with the reorganization shown in eq 4 and also proposed in our earlier work.[2]

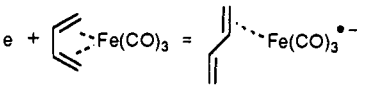

An analogous reorganization is indicated by the present results also for Ol = CHD and CHT. On the other hand, the much smaller bond weakening for (COT)Fe(CO)$_3$ together with the lower $\Delta S°_a$ for that compound suggests that the extra electron is accommodated by a different mechanism, i.e. in an orbital that is not closely associated with bonding. This could be an orbital largely localized on the olefin. Cyclooctatriene is the only ligand amongst the above olefins which has a positive electron affinity. The EA ≈ $-\Delta H_a$ ≈ $-\Delta G°_a$ = 13 kcal/mol for cyclooctatetraene could be measured in the present work, see Figure 1 and Table II. The observation that COT has a sizable electron affinity and thus a low-lying π^* LUMO makes the partial localization of the extra electron in (COT)Fe(CO)$_3^-$ on the COT group much more likely. However, this would have to be confirmed on the basis of a suitable orbital scheme for (COT)Fe(CO)$_3^-$.

Anderson and Symons[19] have obtained ESR spectra of frozen matrices containing (CHD)Fe(CO)$_2$P(Ph)$_3^-$ and observed a large ^{31}P splitting and g values which are consistent with a predominantly metal character of the SOMO. Since the (CHD)Fe(CO)$_2$P(Ph)$_3$ is closely related to the (CHD)Fe(CO)$_3$, these results are consistent with our conclusions above that a metal centered SOMO is present in (CHD)Fe(CO)$_3^-$.

Albright, Geiger, and co-workers[11] were able to observe ESR spectra of frozen solutions of (COT)Fe(CO)$_3^-$ in THF, obtained from the electrochemical reduction of (COT)Fe(CO)$_3$. On the basis of the apparent absence of hyperfine splittings and the g values observed, the authors presented qualitative arguments that the singly occupied orbital (SOMO) is located predominantly on the cyclooctatetraene portion of the radical anion. These conclusions were reinforced by studies of the ESR spectra of (COT)Fe(CO)$_2$P(Ph)$_3^-$ for which the absence of ^{31}P splittings indicated that also for this closely related compound the SOMO is located predominantly on the COT portion of the molecule. Albright and Geiger[11] present also results from extended-Hückel calculations which predict that for (COT)Fe(CO)$_3$, 68% of the LUMO is located on the ligand and the LUMO is concentrated on the uncomplexed portion of the COT ring. These authors provide also interesting information on the predicted hinging angle θ and a very informative qualitative orbital scheme, based on Frontier orbital theory.

More recent work by Golovin and Weaver[20] provides a richer picture for the electrochemical reduction of (COT)Fe(CO)$_3$. These authors studied the cyclic voltammetry of (COT)Fe(CO)$_3$ in the dipolar aprotic solvent acetonitrile and in the protic methanol. FT-IR spectra with a thin layer electrolysis cell were also obtained. The spectrum, after one electron reduction in acetonitrile, indicated that the C≡O stretching frequencies of the radical anion are shifted downwards by ~100 cm^{-1} relative to those in the neutral (COT)Fe(CO)$_3$. The softening of the frequencies was explained on the basis of increased π electron back donation (carbonyl–metal back-bonding) which would be expected for a SOMO that has significant metal character. On the other hand in the protic methanol the results were consistent with an irreversible two electron reduction which consumes also two protons and led to a hydrogenation of one of the double bonds in the COT ring. Since information on the one electron reduced

(17) Engleking, P. C.; Lineberger, W. C. *J. Am. Chem. Soc.* **1979**, *101*, 5569.

(18) Sunderlin, L. S.; Wang, D.; Squires, R. R. *J. Am. Chem. Soc.* **1992**, *114*, 2788. The quoted bond energies from the above authors are probably more reliable than the values D(Bd–Fe(CO)$_3$) = 47.8 kcal/mol and D(COT–Fe(CO)$_3$) = 42.3 kcal/mol, which are based on earlier determinations, see: Martinhoe-Simoes, J. A.; Beauchamp, J. L. *Chem. Rev.* **1990**, *90*, 629. Brown, D. L. S.; Connor, J. A.; Leung, M. L.; Paz-Andrade, M. I.; Skinner, H. A. *J. Organomet. Chem.* **1976**, *110*, 79. Connor, J. A.; Demain, C. P.; Skinner, H. A.; Zaffarami-Moattaz, M. T. *J. Organomet. Chem.* **1979**, *170*, 117.

(19) Anderson, O. P.; Symons, M. C. R. *Inorg. Chem.* **1973**, *12*, 1932.

(20) Golovin, M. N.; Weaver, M. J. *Inorg. Chim. Acta* **1988**, *142*, 177.

(21) (a) Grimsrud, E. P.; Chowdhury, S.; Kebarle, P. *J. Chem. Phys.* **1985**, *83*, 1059. (b) Chowdhury, S.; Kebarle, P. *J. Chem. Phys.* **1986**, *85*, 4985.

(22) Richardson, D. E. *J. Phys. Chem.* **1986**, *90*, 3697.

Table III. Electron-Transfer Rate Measurements[a]

reactant	$-\Delta G°_a$(A)(373 K)	$\Delta G°_{el}$	log k
	BdFe(CO)$_3$		
C_6F_6	14.4[b]	−10.2	−8.60
4CF$_3$-NB	18.5[c]	−6.1	−9.32
2,3-(CH$_3$)$_2$-NB	19.5[d]	−5.1	−10.32
NB	22.9[e]	−1.7	−11.46
2F-NB	24.3[e]	−0.3	−11.20
3F-NB	27.8[e]	3.2	−11.06
3CF$_3$-NB	31.7[e]	7.1	−10.14
2CHO-NB	34.7[c]	10.1	−9.86
(CH$_3$)$_4$Qu	36.2[d]	11.6	−9.82
NpQu	40.4[e]	15.8	−9.65
	(CHD)Fe(CO)$_3$		
3CF$_3$-BN	15.4[g]	−6.6	−9.17
4CF$_3$-BN	18.5[h]	−3.5	−9.69
4CH$_3$-NB	21.3[e]	−0.7	−11.38
3CH$_3$-NB	22.2[e]	0.2	−11.34
NB	22.9[e]	0.9	−11.43
3F-NB	27.8[e]	5.8	−10.38
3CF$_3$-NB	31.7[e]	9.7	−9.53
4CH$_3$-CO-NB	34.9[c]	12.9	−9.39
	(CHT)Fe(CO)$_3$		
4CF$_3$-BN	18.5[h]	−8.4	−8.82
4CH$_3$-NB	21.3[e]	−5.6	−9.12
3CH$_3$O-NB	23.5[d]	−3.4	−9.35
2F-NB	24.3[e]	−2.6	−9.60
3F-NB	27.8[e]	0.9	−9.97
3CF$_3$-NB	31.7[e]	4.8	−9.62
4AcNB	34.9[c]	8.0	−9.41
1,3-diNB	37.0[e]	10.2	−9.32
	(COT)Fe(CO)$_3$		
2F-NB	24.3[e]	−8.7	−8.99
t-(CN)$_2$C$_2$H$_2$	28.5[h]	−4.5	−8.72
3CH$_3$CO-NB	29.4[c]	−3.6	−9.08
2CF$_3$-NB	30.0[c]	−3.0	−8.98
3CF$_3$-NB	31.7[e]	−1.3	−8.96[d]
2CHO-NB	34.7[c]	1.7	−8.96
NpQu	40.4[e]	7.4	−9.03
	(CHT)Cr(CO)$_3$		
3CF$_3$-BN	15.4[g]	−7.9	−8.67
2,3-(CH$_3$)$_2$-NB	19.5[d]	−3.8	−9.00
4CH$_3$-NB	21.3[e]	−2.0	−9.00
2F-NB	24.3[e]	1.0	−8.94
4F-NB	25.1[e]	1.8	−8.90
3F-NB	27.8[e]	4.5	−8.94
3CF$_3$-NB	31.7[e]	8.4	−8.73

[a] Rate constant for electron-transfer reactions $A^- + B = A + B^-$ involving organometallic compound B heading each table and reference compounds A. $\Delta G°_{el}$ relate to the electron-transfer reaction above. Rate constants k always were measured in the exoergic direction. Thus for cases where $\Delta G°_{el}$ is positive, the rate was measured for the reverse reaction: $B^- + A = B + A^-$. Energies in kcal/mol. Rates were measured at 373 K. Notation for reference compounds A: NB = nitrobenzene; BN = benzonitrile; Qu = quinone; NpQu = naphthoquinone; 1,3-diNM = 1,3-dinitrobenzene. [b] Value of $\Delta G°_a$(373 K) obtained from $\Delta G°_a$(423 K) and $\Delta S°_a$, which are given in: Chowdhury, S.; Grimsrud, E. P.; Heinis, T.; Kebarle, P. *J. Am. Chem. Soc.* **1986**, *108*, 3630. [c] Value of $\Delta G°_a$(373 K) obtained from $\Delta G°_a$(423 K) and estimated value of $\Delta S°_a$, which are given in: Chowdhury, S.; Kishi, H.; Dillow, G. W.; Kebarle, P. *Can. J. Chem.* **1988**, *67*, 603. [d] Value of $\Delta G°_a$(373 K) obtained from $\Delta G°_a$(423 K) and value of $\Delta S°_a$, which was estimated to be −2 eu, typical for substituted nitrobenzenes (see references in footnotes *c* and *h*). [e] Value of $\Delta G°_a$(373 K) obtained from $\Delta G°_a$(423 K) and $\Delta S°_a$, which are given in Heinis et al. (Heinis, T.; Chowdhury, S.; Scott, S. L.; Kebarle, P. *J. Am. Chem. Soc.* **1986**, *90*, 2747). [f] Value of $\Delta G°_a$(373 K) obtained from $\Delta G°_a$(423 K) and $\Delta S°_a$, which are given in Heinis et al. (Heinis, T.; Chowdhury, S.; Scott, S. L.; Kebarle, P. *J. Am. Chem. Soc.* **1988**, *100*, 400). [g] Value of $\Delta G°_a$(373 K) obtained from $\Delta G°_a$(423 K) given in Chowdhury et al. (Chowdhury, S.; Kebarle, P. *J. Am. Chem. Soc.* **1986**, *108*, 5453) and assuming a value of $\Delta S°_a$ of +2.8 eu, which was determined for the para isomer in the same report. [h] Value of $\Delta G°_a$(373 K) obtained from $\Delta G_a°$(423 K) and $\Delta S°_a$, determined in the reference in footnote *g* above.

species in methanol is not available, a detailed interpretation of the Weaver results appears difficult. However, we believe that

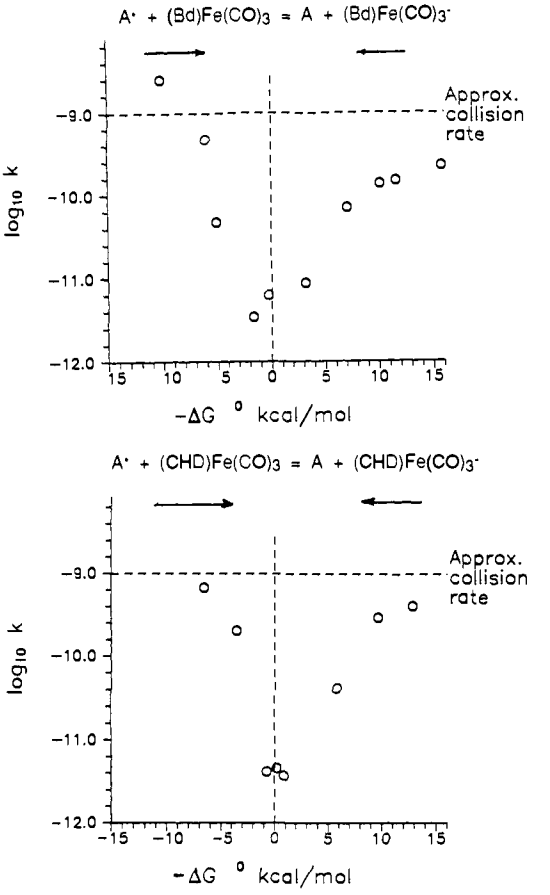

Figure 3. (I, top) Dependence of rate of electron transfer on exoergicity of the reaction $A^- + BdFe(CO)_3 = A + BdFe(CO)_3^-$. Various compounds A with different $\Delta G°_a$ were used such that the reaction was exoergic from left to right, see rate constants under →. With another group of A compounds reaction was exoergic from right to left, see rate constants under ←. Only rates in the exoergic direction were measured. (II, bottom) Same as above but for the reaction $A^- + (CHD)Fe(CO)_3 = A + CHDFe(CO)_3^-$.

the results indicate that the SOMO character in (COT)Fe(CO)$_3^-$ is solvent dependent. This should also mean that the radical anion structures with a largely metal centered SOMO or a largely COT centered SOMO are of similar energies.

The ESR results of Albright and Geiger[11] and the FT-IR results of Golovin and Weaver[19] on (COT)Fe(CO)$_3^-$ are not completely concordant. However, both studies indicate that for this ligand an olefin centered SOMO becomes a likely possibility. Thus they conform with the conclusions based on the present thermochemical data which indicate that a changeover from a metal character SOMO to an olefin ligand SOMO occurs for the ligand series Bd, CHD, CHT, and COT when COT is reached.

It is interesting to compare the electron attachment data, $\Delta H°_a$ and $\Delta S°_a$, for the OlFe(CO)$_3$ series with that for (CHT)Cr(CO)$_3$, which were also obtained in the present work, see Figure 1, Table I, and the structure below:

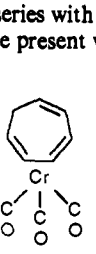

(CHT)Cr(CO)$_3$

$\Delta H°_a$ = 21.4 kcal/mol; $\Delta S°_a$ = +5.0 cal K^{-1} mol^{-1}

Cr has 6 valence electrons, 2 less less than Fe, and thus (CHT)Cr(CO)$_3$ as an 18-electron species is η^6-(CHT)Cr(CO)$_3$. One may consider that on capture of an electron, the coordination decreases to η^4-CHTCr(CO)$_3$ and the extra electron enters the newly created LUMO as was the case for Bd, CHD, and CHT

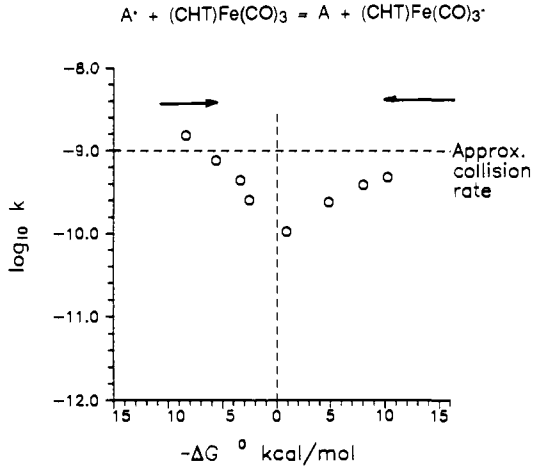

Figure 4. Same as in Figure 3 but for the reaction $A^- + CHTFe(CO)_3 = A + CHTFe(CO)_3^-$.

iron tricarbonyls. The much lower $\Delta S°_a = +5$ cal K^{-1} mol^{-1} for the Cr compound compared to $\Delta S°_a \approx 10$ cal K^{-1} mol^{-1} for the Fe complexes is consistent with such a process. A large entropy gain will occur only when a significant loosening of the bonding between the olefin and the metal tricarbonyl occurs, such that "soft" frequencies in the 100–500 cm^{-1} wavenumber range are created. Since for the case of Cr there is still at least a two π bond coordination present in the radical anion, soft motions will not have been created on electron capture to the same extent as for the Fe species where the coordination falls to one π bond in the anion.

We have assumed above that the bond weakening in the Ol-$Fe(CO)_3^-$ complexes where Ol = Bd, CHD, and CHT is due to a break of a Fe–ligand bond, i.e. a reduction of hapticity form four to two. It is possible that such a drastic orbital and structural reorganization is not required to accommodate the extra electron. Thus a tetrahaptomonoanion where the SOMO is antibonding between the metal and the polyolefin could also account for the bond weakening. Since the thermodynamic data obtained with our experiments do not provide direct information on structure, we cannot give a definitive answer on this point. The large $\Delta S°_a$ observed for the above Ol-$Fe(CO)_3$ complexes are indicative of significant geometry reorganization on electron capture. As will be shown in the next section on the kinetics of electron transfer, the kinetic results also indicate large geometry changes for Ol = Bd, CHD, and CHT but a small change for COT. We assume that these large changes are more consistent with a change of hapticity and the interpretation of Krusic[5] than with a bond weakening due to the electron entering an antibonding LUMO.

b. Rates of Electron Transfer and Reorganization on Electron Capture. Previous studies[21,22] of the kinetics of gas phase electron transfer reactions 2 showed that these proceed at collision rates

$$A^- + B = A + B^- \qquad (2)$$

when the reactions are exoergic and when the geometry changes between A and A^- and B and B^- are small. On the other hand, exoergic reactions where the geometry changes for either A,A^- or B,B^-, or both, are appreciable proceed below collision rates and the rates increase as the exoergicity of the reaction increases. This behavior is predicted by the Marcus equation.[23] The quantitative application of theory to gas phase electron transfer reactions is not very advanced, and some specific problems and solutions have been described.[21,22,24] Qualitatively, it is possible to use the measured rates and their dependence on the exoergicity of the reaction to obtain a measure for the geometry changes occurring in the reactants. By selecting reference compounds A for which

(23) Sutin, N. *Prog. Inorg. Chem.* **1983**, *30*, 441. Marcus, R. A.; Sutin, N. *Inorg. Chem.* **1975**, *14*, 213.

(24) Han, C. C.; Wibbur, J. L.; Brauman, J. I. *J. Am. Chem. Soc.* **1992**, *114*, 887.

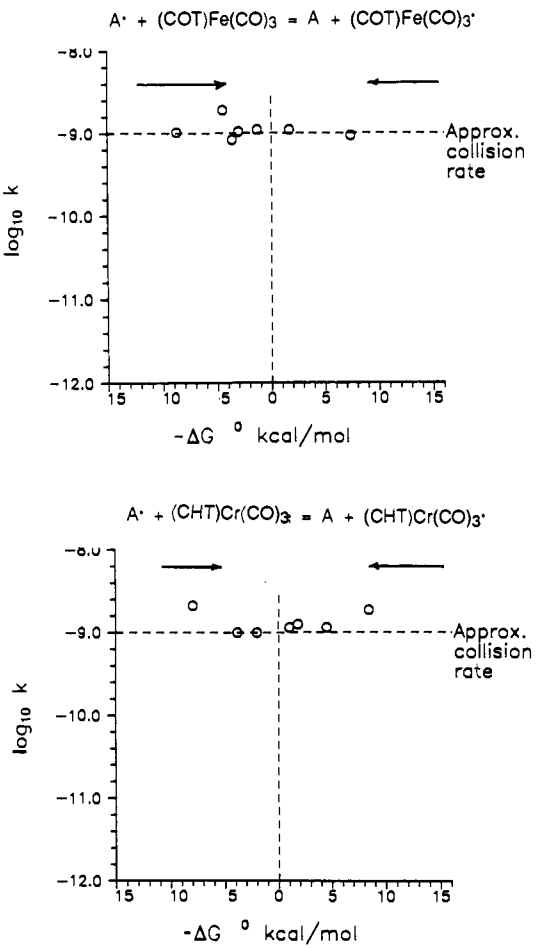

Figure 5. Same as in Figure 3 but for the reactions $A^- + COTFe(CO)_3 = A + COTFe(CO)_3^-$ and $A^- + CHTCr(CO)_3 = A + CHTCr(CO)_3^-$.

it is known that the geometry changes A,A^- are small, the measured rate dependence on the exoergicity becomes a qualitative measure of the geometry changes B,B^- where, for the present case, B are the organometallic compounds of interest. Compounds A with small geometry changes are selected both on the basis of a small $\Delta S°_a$(A) and the fact that these reactants when involved in electron transfer with other compounds (with small geometry change) lead to electron transfer at collision rates.

Rate constants k_2 for a given B = (Bd)$Fe(CO)_3$, (CHD)Fe-$(CO)_3$, (CHT)$Fe(CO)_3$, (COT)$Fe(CO)_3$, and (CHT)$Cr(CO)_3$ reacting with a variety of reference compounds A such that reactions of a wide exoergicity range are covered were determined in the present work. For methodology, see Experimental Section and Dillow.[2] The rate constant values obtained are given in Table III and Figures 3–5.

The results present an interesting and independent confirmation of the conclusions reached in the discussion of the thermodynamic data. Thus (Bd)$Fe(CO)_3$ and (CHD)$Fe(CO)_3$, for which the electron attachment entropy increases were the largest (10.2 and 11.4 cal K^{-1} mol^{-1}) and the bond energy decreases (see cycle 8 and eq 9) were also the largest (21 and 24 kcal/mol), exhibit the largest decreases of rate constants at zero exoergicity, see Figure 3. Thus, these results which indicate large geometry changes on formation of the negative ions are consistent with the conclusions in the preceding section of the Discussion.

For (CHT)$Fe(CO)_3$ which showed a somewhat intermediate behavior, but was closer to (Bd)$Fe(CO)_3$ and (CHD)$Fe(CO)_3$, the rate data (Figure 4) show a smaller dip in rates at near zero exoergicities. It should be recalled that in the gas phase, the lowering of the energy due to ion–molecule polarizability and dipole interactions is generally quite large. Therefore, the energy barrier associated with the formation of the transition state must

be also quite high before a slowdown below collision rates is observed for gas phase ion–molecule reactions.[2,21-24] Therefore, although the dip in the rate constant plot for $(CHT)Fe(CO)_3$ is smaller than those for Bd and CHD shown in Figure 3, still a substantial geometry change is indicated by the plot.

The rate constant plots for $(COT)Fe(CO)_3$ and $(CHT)Cr(CO)_3$, shown in Figure 5, exhibit essentially no decrease of rates at near zero exoergicities. A very small dip would be expected from the consideration that the forward rate should go down to half of the collision rate when the exoergicity is exactly equal to zero. Thus, the results in Figure 5 are consistent with the small $\Delta S°_a$ for $(COT)Fe(CO)_3$ and $(CHT)Cr(CO)_3$ of 8.7 and 5 cal K^{-1} mol^{-1}, Table II, and the expected small geometry changes deduced in the preceding section from the observed changes of bonding in the neutral molecule and the negative ion.

Acknowledgment. Financial support by the Canadian Natural Sciences and Engineering Research Council is gratefully acknowledged.

Communications to the Editor

Metalation of Imines by Lithium Diisopropylamide Solvated by *N,N,N',N'*-Tetramethylethylenediamine: Evidence for Solvent-Free Open Dimer Reactive Intermediates

Max P. Bernstein and David B. Collum*

Baker Laboratory, Department of Chemistry
Cornell University, Ithaca, New York 14853-1301

Received September 14, 1992

Previous rate studies of *N,N*-dimethylhydrazone metalations by LDA in THF/hexane or TMEDA/hexane (TMEDA = *N,N,N',N'*-tetramethylethylenediamine) implicated mechanisms involving deaggregation of LDA dimers without participation by additional donor solvent (eq 1, R_1 = Me, R_2 = NMe_2).[1,2] We concluded that TMEDA functions as a monodentate rather than bidentate ligand in both the ground state (e.g., **1**) and the transition state.[2] Furthermore, the surprisingly low affinity of TMEDA for LDA led us to question the mode of action of TMEDA as a ligand for lithium in a more general sense.[3] In this communication we will provide evidence that LDA/TMEDA-mediated metalations of simple *N*-isopropyl imine **2** proceed by a mechanism involving a dimer–monomer pre-equilibrium akin to that observed for the isostructural *N,N*-dimethylhydrazones. In contrast, metalation of imine **3** bearing a pendant NMe_2 moiety is extremely rapid and proceeds by a mechanism involving facile dissociation of *both* TMEDA ligands from LDA dimer **1** followed by direct reaction of the LDA dimer. We ascribe the change in the rate equation to the Me_2N moiety. The kinetics provide clear evidence of a ligand-assisted metalation (complex-induced proximity effect; CIPE)[4] and gives experimental support to speculations that lithium amide open dimers may be important reactive intermediates.[5-7]

Metalations of imine **2** and the 2,2,6,6-tetradeuterio derivative **2**-d_4 by LDA in TMEDA/hexane mixtures, maintained at 0 °C

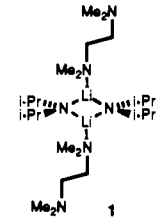

1

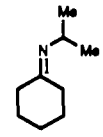

2

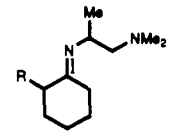

3; R = Me
4; R = H

with an ice bath, were monitored using an FT-IR continuous-flow method described previously.[1,2] The primary kinetic isotope effect (k_H/k_D = 7.7 ± 1.0) and rate equation (eq 2) are consistent with a mechanism involving dimer dissociation (eq 1, R_1 = H, R_2 = $CHMe_2$).[1,2] Moreover, the completely analogous rate equations for metalation of *N,N*-dimethylhydrazones and *N*-isopropyl imines indicate that the Me_2N moieties of the hydrazones do *not* function as obligatory ligands during the metalation.

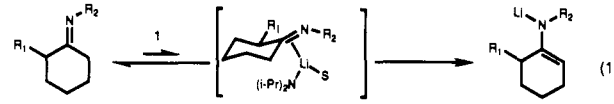

(1)

$$-d[2]/dt = k'[\text{substrate}][LDA]^{1/2}[TMEDA]^0 \qquad (2)$$

We investigated the possibility that inclusion of a second ligand on the imine *N*-alkyl substituent might, through chelation, cause an increased metalation rate characteristic of a CIPE.[4] Such a CIPE should be accompanied by a fundamental change in the mathematical form of the rate equation. The metalations of **4** and **4**-d_4 proved to be too fast to monitor within the restrictions of the continuous-flow IR cell, clearly demonstrating that the pendant Me_2N of **4** facilitates the metalation relative to **2**. Fortunately, reduced metalation rates of the methylated derivatives **3** and **3**-d_3 allowed for reasonably precise rate measurements.[10] An unusually small kinetic isotope effect (k_H/k_D = 2.0 ± 0.1) was accompanied by a substantial change in the rate equation (eq 3).[8] The first-order dependence on [LDA] and first-order dependence on [**3**][9] implicate a direct metalation by the intact LDA dimer fragment. The inverse second-order dependence on [TMEDA] (Figure 1) causes a striking exponential increase in metalation rate with decreasing TMEDA concentration and points to a mechanism involving dissociation of *both* η^1-TMEDA ligands prior to metalation. In previous studies we had shown that THF is superior to TMEDA as a ligand for LDA. Indeed, addition of 2% by volume THF to metalations of **3** in TMEDA or TME-

(1) Galiano-Roth, A. S.; Collum, D. B. *J. Am. Chem. Soc.* **1989**, *111*, 6772.
(2) Bernstein, M. P.; Romesberg, F. E.; Fuller, D. J.; Harrison, A. T.; Collum, D. B.; Liu, Q.-Y.; Williard, P. G. *J. Am. Chem. Soc.* **1992**, *114*, 5100.
(3) Collum, D. B. *Acc. Chem. Res.* **1992**, *25*, 448.
(4) For detailed discussions of complex-induced proximity effects, chelation effects, and other synonymous influences of internal ligation, see: Beak, P.; Meyers, A. I. *Acc. Chem. Res.* **1986**, *19*, 356. Hay, D. R.; Song, Z.; Smith, S. G.; Beak, P. *J. Am. Chem. Soc.* **1988**, *110*, 8145. Gronert, S.; Streitwieser, A., Jr. *J. Am. Chem. Soc.* **1988**, *110*, 2843. Chen, X.; Hortelano, E. R.; Eliel, E. L.; Frye, S. V. *J. Am. Chem. Soc.* **1992**, *114*, 1778. Das, G.; Thornton, E. R. *J. Am. Chem. Soc.* **1990**, *112*, 5360. Klumpp, G. W. *Recl. Trav. Chim. Pays-Bas* **1986**, *105*, 1. van Eikema Hommes, N. J. R.; Schleyer, P. v. R. *Angew. Chem., Int. Ed. Engl.* **1992**, *31*, 755.
(5) Romesberg, F. E.; Gilchrist, J. H.; Harrison, A. T.; Fuller, D. J.; Collum, D. B. *J. Am. Chem. Soc.* **1991**, *113*, 5751.
(6) Romesberg, F. E.; Collum, D. B. *J. Am. Chem. Soc.* **1992**, *114*, 2112.
(7) The open dimer of lithium 2,2,6,6-tetramethylpiperidide (LiTMP) bearing a single chelating TMEDA ligand has been characterized: Nichols, M. A.; Williard, P. G. Unpublished results.
(8) Bell, R. P. *The Proton in Chemistry*; Cornell University Press: Ithaca, NY, 1973; Chapter 12.
(9) The independence of the measured rate constants on imine concentration and the high quality of the nonlinear least-squares fits clearly demonstrate the reaction orders for imines **2** and **3** to be unity. Although the two diastereomers of **3** must react at different rates, these differences appear to be well within experimental error.

0002-7863/93/1515-789$04.00/0